

Annual Review of Marine Science

Aquatic Eddy Covariance: The Method and Its Contributions to Defining Oxygen and Carbon Fluxes in Marine Environments

Peter Berg,¹ Markus Huettel,² Ronnie N. Glud,^{3,4} Clare E. Reimers,⁵ and Karl M. Attard³

- ¹Department of Environmental Sciences, University of Virginia, Charlottesville, Virginia 22908, USA; email: pb8n@virginia.edu
- ²Department of Earth, Ocean, and Atmospheric Science, Florida State University, Tallahassee, Florida 32306, USA; email: mhuettel@fsu.edu
- ³ Danish Center for Hadal Research (HADAL), Nordic Center for Earth Evolution (NordCEE), Danish Institute for Advanced Study (DIAS), and Department of Biology, University of Southern Denmark, DK-5230 Odense M, Denmark; email: rnglud@biology.sdu.dk, karl.attard@biology.sdu.dk
- ⁴Department of Ocean and Environmental Sciences, Tokyo University of Marine Science and Technology, Tokyo 108-8477, Japan
- ⁵College of Earth, Ocean, and Atmospheric Sciences, Oregon State University, Corvallis, Oregon 97331, USA; email: clare.reimers@oregonstate.edu

ANNUAL CONNECT

www.annualreviews.org

- Download figures
- · Navigate cited references
- Keyword search
- · Explore related articles
- · Share via email or social media

Annu. Rev. Mar. Sci. 2022. 14:431-55

First published as a Review in Advance on September 29, 2021

The *Annual Review of Marine Science* is online at marine.annualreviews.org

https://doi.org/10.1146/annurev-marine-042121-012329

Copyright © 2022 by Annual Reviews. All rights reserved

Keywords

aquatic eddy covariance, oxygen dynamics, carbon cycling, blue carbon, drivers of oxygen flux, sediment-water exchange, air-water exchange

Abstract

Aquatic eddy covariance (AEC) is increasingly being used to study benthic oxygen (O_2) flux dynamics, organic carbon cycling, and ecosystem health in marine and freshwater environments. Because it is a noninvasive technique, has a high temporal resolution (\sim 15 min), and integrates over a large area of the seafloor (typically 10–100 m²), it has provided new insights on the functioning of aquatic ecosystems under naturally varying in situ conditions and has given us more accurate assessments of their metabolism. In this review, we summarize biogeochemical, ecological, and biological insights

gained from AEC studies of marine ecosystems. A general finding for all substrates is that benthic $\rm O_2$ exchange is far more dynamic than earlier recognized, and thus accurate mean values can only be obtained from measurements that integrate over all timescales that affect the local $\rm O_2$ exchange. Finally, we highlight new developments of the technique, including measurements of air—water gas exchange and long-term deployments.

1. OXYGEN FLUXES: A ROBUST PROXY FOR CARBON TRANSFORMATIONS

In terrestrial and aquatic ecosystems, there is usually a near-1:1 match between rates of biologically driven photosynthetic carbon fixation and coupled oxygen (O_2) production and between respiratory carbon oxidation and O_2 consumption. This stochiometric equivalence and the fact that O_2 is relatively easy to measure have made O_2 fluxes the most used proxy for studying inorganic—organic carbon (C) transformations in aquatic systems.

Marine sediments cover approximately 70% of Earth's solid surface and are critically important sites for the deposition and respiration of organic carbon (org-C) originating from marine and terrestrial plants. Typically, aerobic respiration dominates in deep-sea settings, whereas coastal sediments host significant levels of anaerobic respiration (Canfield et al. 1993, Jørgensen 1982, Thamdrup 2000). Although the 1:1 O₂:C stochiometric equivalence usually holds for both direct aerobic org-C respiration and indirect aerobic reoxidation of reduced compounds from anaerobic org-C respiration (Glud 2008), different O₂:C exchange ratios are found in some settings, including sites with high nitrification levels, substantial burial of reduced products of anaerobic mineralization, and considerable denitrification that releases reduced nitrogen as dinitrogen to the water column. In addition, sediments exposed to significant seasonal deposition dynamics or hypoxia may temporarily accumulate reduced compounds and induce a time lag between ongoing benthic org-C mineralization and the associated benthic O₂ uptake. This temporal misalignment, or O₂ debt (Pamatmat 1971), diminishes when the O₂ uptake is integrated over time. Finally, in light-exposed substrates hosting photosynthetic C fixation, processes like photorespiration and light inhibition can skew the 1:1 equivalence some. In summary, however, the usually tight 1:1 relationship between rates of benthic respiration and photosynthetic production and the parallel uptake or release of O₂ enable us to determine the net effects of these two fundamental processes by measuring benthic O₂ exchange rates.

For decades, benthic O_2 fluxes have been measured in recovered sediment cores incubated in controlled environments mimicking in situ conditions (Hayes & MacAulay 1959, Mortimer 1941) and in in situ chambers that isolate only a small area of the sediment surface (Odum 1957, Pamatmat & Fenton 1968). Limitations of these still widely used flux methods include that they disturb the substrate and exclude or seriously alter the natural ecosystem-scale drivers of O_2 flux (e.g., flow, light, and org-C and nutrient exchange with the water column). They are, additionally, challenging to implement for a number of substrates, including highly permeable sands, hard substrates, and seagrass beds.

This review describes how aquatic eddy covariance (AEC) has been developed and applied to overcome these challenges and how AEC studies have provided new insights on the biogeochemical functioning of numerous aquatic substrates. AEC is a general, direct, and noninvasive underwater flux method that is applicable to any scalar quantity that can be measured at a point and at a rate fast enough to capture turbulent fluctuations. We have, however, limited this review to focusing on O_2 exchange in marine ecosystems.

2. AQUATIC EDDY COVARIANCE

2.1. Historical Background

The theoretical foundation for eddy covariance was formulated by Reynolds (1895) decades before the required instrumentation was developed. According to Baldocchi (2003), the very first measurements were made in the atmosphere by Scrase (1930), who determined the transport of momentum (Reynolds stress) using simple analog instrumentation and strip-chart data recording. Years later, groundbreaking inventions in fast-responding hot-wire anemometry (Priestley & Swinbank 1947, Swinbank 1951) kick-started the development of eddy covariance in air (Baldocchi 2013), which is today by far the most used flux method for measuring the atmospheric exchange of many constituents with terrestrial substrates.

Underwater, the first uses of AEC measured water column salt fluxes in an estuary (Partch & Smith 1978) and heat fluxes under sea ice (McPhee 1992). Later, Berg et al. (2003) showed that O₂ fluxes between benthic substrates and the water column above can be measured consistently by AEC. Due to the already widespread use of benthic O₂ exchange rates in marine ecology and a demand for better approaches, this study motivated others to adapt and further develop the AEC technique.

2.2. Basic Principles

Dissolved O_2 can be transported in water by advection and molecular diffusion. The universal expression for the instantaneous vertical O_2 flux yields

$$flux = wC - D\frac{dC}{dz},$$
1.

where w is the vertical flow velocity, C the O_2 concentration, D the molecular diffusivity of O_2 in water, and z the vertical coordinate. Away from millimeter-scale diffusive boundary layers that overlay impermeable surfaces, and outside environments with extreme density gradients, the diffusive term, D(dC/dz), can be neglected.

In his famous paper, Reynolds (1895) proposed that an observed value in a turbulent flow (e.g., w or C; Equation 1) can be expressed as a mean plus a turbulent fluctuation away from the mean (e.g., $w = \bar{w} + w'$ or $C = \bar{C} + C'$). This separation is referred to as Reynolds decomposition, and using it for both w and C in Equation 1 gives an expression for the averaged flux of

$$\overline{\text{flux}} = \overline{\overline{w}\overline{C}} + \overline{\overline{w}C'} + \overline{w'\overline{C}} + \overline{w'C'} .$$
 2.

Assuming that the averaging time is long enough for the averages of the fluctuating components, $\overline{w'}$ and $\overline{C'}$, to equal zero, and that the coordinate system is perpendicular to the flow streamlines so that \overline{w} equals zero, gives

$$\overline{\text{flux}} = \overline{w'C'}$$
.

This is the fundamental expression in AEC, stating that the so-called eddy flux—the averaged vertical O_2 flux in the water column down toward or up from a benthic substrate—can be derived from direct, fast point measurements of w and C (Figure 1).

2.3. Field Measurements and Instrumentation

The eddy flux (Equation 3) determined for a fixed point above a benthic surface is usually an accurate representation of the benthic flux between the seafloor and the water above. One condition for this equivalence is that the consumption and photosynthetic production of O_2 in the water column between the seafloor and the measuring point must be insignificant compared with the

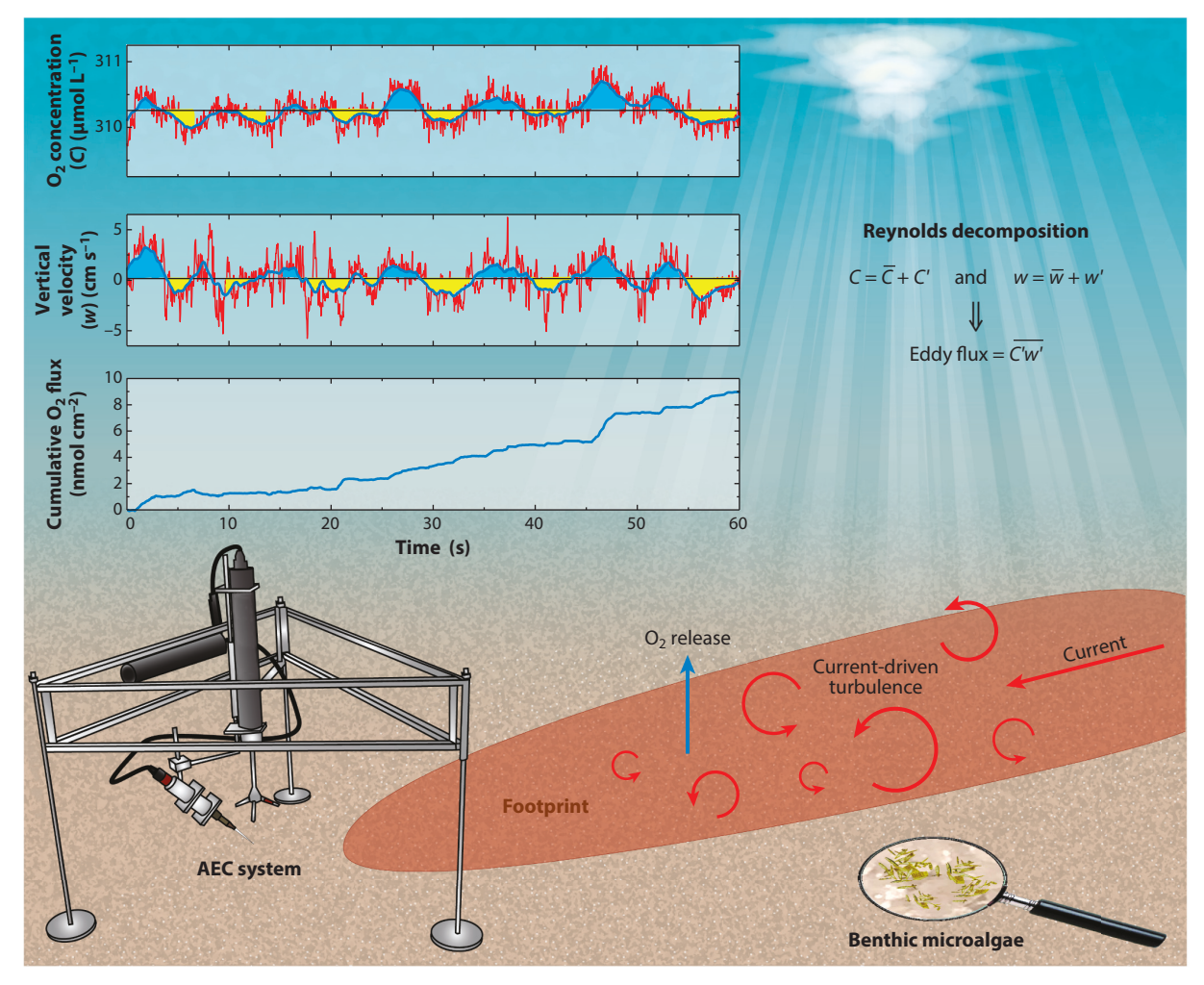


Figure 1

An AEC system (lower left) collecting data over a light-exposed seafloor that releases O_2 due to photosynthesizing benthic microalgae (lower right). The seafloor area producing the eddy flux signal is referred to as the footprint and is located upstream from the system (red shading). Three graphs (upper left) show 1 min of fast measurements (8 Hz) of the fluctuating O_2 concentration (C, top), the fluctuating vertical velocity (w, middle), and the cumulation of the instantaneous flux (bottom). During periods marked with yellow, the vertical velocity is directed down, and the O_2 concentration is below average. During periods marked with blue, the velocity is directed up, and the O_2 concentration is above average. This highly dynamic but persistent turbulent pattern will, when averaged over time, give a net transport of O_2 up from the benthic substrate. The linear trend of the cumulative O_2 flux indicates a strong flux signal in the data. Abbreviation: AEC, aquatic eddy covariance. AEC system drawing by Luke Cole, University of Virginia.

benthic flux. Also, rapid changes in mean current velocity or mean water column O₂ concentration can skew this equivalence for short periods (Holtappels et al. 2013). Such effects diminish if the integration time is extended, and biases due to both effects are minimized if the measuring point is located close to the seafloor. However, the measuring point must be positioned high enough above the benthic surface to ensure that the turbulence and the eddy flux signal represent the substrate as a whole and not just a few larger objects on the seafloor (Rheuban & Berg 2013). The best compromise between these diverging factors depends on the environment and substrate

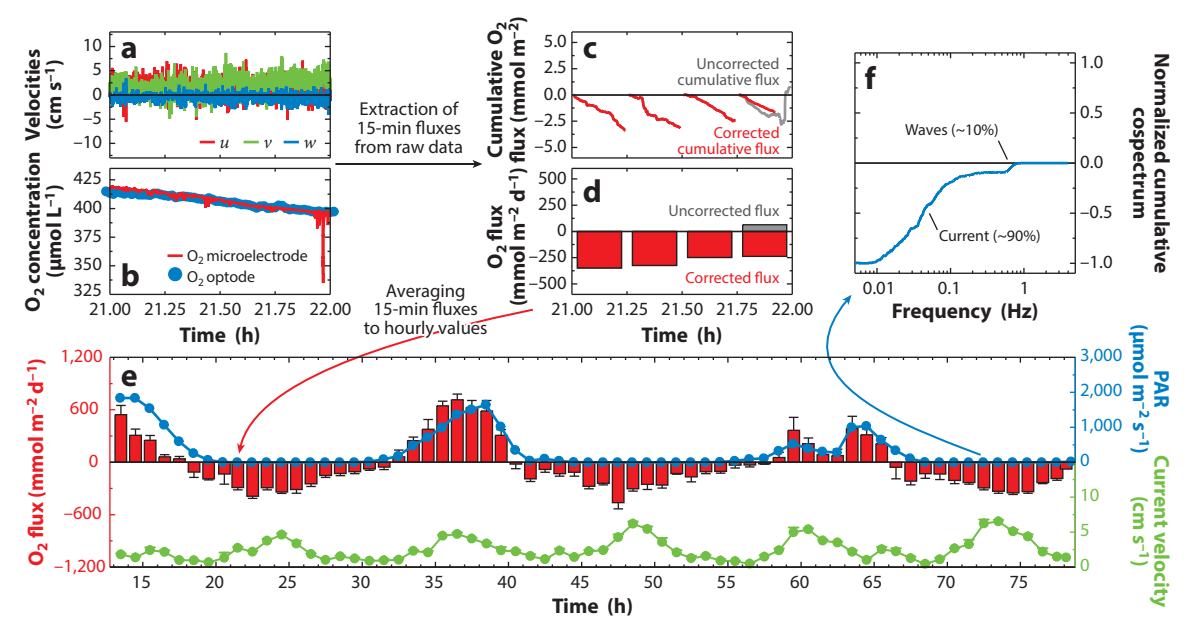


Figure 2

Example of AEC data and their processing. The data cover 2.7 days and were measured in a seagrass meadow. (a) Three-dimensional velocity data (w is vertical) at 8 Hz through 1 h. (b) Matching O₂ concentrations recorded with a Clark-type microelectrode and an independent optode. Attached debris temporarily disturbed the microelectrode signal at the end of the data sequence. (ϵ) Extracted cumulative O₂ fluxes for 15-min time intervals. (d) Matching 15-min fluxes (negative fluxes represent an uptake). Data shown in gray include the disturbed microelectrode signal. Such compromised data can result in significant errors in flux extraction and are removed when data are processed. (ϵ) Hourly averages of 15-min O₂ fluxes, light (PAR), and current velocity. Error bars represent standard errors. A tight modulation of the O₂ flux by light during daytime is evident, while significant stimulation of seagrass meadow uptake by current velocity is seen at nighttime. (f) Normalized cumulative cospectrum of the O₂ flux signal for 1 h of data. The spectrum reveals that the entire eddy flux signal was associated with frequencies of <0.8 Hz and that wave motions (0.5–0.8 Hz) here facilitated only a small fraction of the total O₂ flux. Abbreviations: AEC, aquatic eddy covariance; PAR, photosynthetically active radiation. Panel ϵ adapted from Berger et al. (2020).

roughness, but most studies to date have used measuring heights between 5 and 30 cm (Berg et al. 2017).

Usually 15 min of data are adequate to produce one statistically sound flux estimate (Berg et al. 2003). Sometimes derived fluxes are further averaged to hourly exchange rates before further analysis (Hume et al. 2011) (**Figure 2**).

The universally used instrument for measuring water velocities for AEC is the acoustic Doppler velocimeter (ADV) named the Vector (Nortek, Norway). This instrument measures the three-dimensional velocity field at frequencies up to 64 Hz and can additionally record two external signals on its internal data logger. Using this feature to record the O₂ sensor signal ensures that all data are aligned perfectly in time (Berg et al. 2015, Lorrai et al. 2010). An 8-Hz data resolution is usually sufficient to describe all fluctuations contributing to the eddy flux, but a higher recording frequency (e.g., 32 or 64 Hz) is often used to allow noise reduction by down-averaging (Berg et al. 2009).

Early AEC studies measured the O_2 concentration exclusively with Clark-type microelectrodes (Revsbech 1989) that are fast-responding (90% response time of 0.2–0.4 s) and typically have a thin tip (10–50 μ m). This sensor, however, is fragile and breaks easily if floating debris or fauna collide with the tip. Although thicker and sturdier Clark-type microelectrodes can be produced

for AEC measurements, alternatives have been developed and tested, including more robust fiber-optical O_2 sensors (Chipman et al. 2012) that have comparable response times, a tip diameter of $100-500~\mu m$, and deployment lifetimes that usually exceed those of microelectrodes (Huettel et al. 2020). Another alternative is a dual O_2 -temperature sensor specially developed for parallel AEC measurements of O_2 and heat fluxes (Berg et al. 2016). Its large tip (8 mm) consists of a miniature planar O_2 optode and a microthermistor, and it is the most robust commercially available AEC sensor. The sensor is best suited for settings where it can be oriented relative to a predictable flow direction because its large tip can distort the velocity measurements if it is positioned directly upstream from the ADV (Berg et al. 2016, Huettel et al. 2020). An alternative specialized sensor setup relies on pumping water through a thin sample line into a flow-through cell that contains one or two fast-responding sensors (Long 2021, Long et al. 2015c). An advantage of this design is that it ensures uniform working conditions for the sensors with respect to flow and light interference, but it adds to the response time of the concentration readings and is susceptible to clogging in some environments.

The ADV and the O₂ sensor are typically mounted at a fixed point above the seafloor on a light, thin-legged frame to minimize disturbances of flow and light (Attard et al. 2020, Berg & Huettel 2008, Huettel et al. 2020). Heavier frames have been used in shelf environments with high-energy flows to ensure platform stability (Reimers et al. 2012). A more complex precursor to these fixed frames was designed to detect the current direction from ADV readings and, driven by a computer-controlled motor, to rotate in the horizontal plane every 15 min to orient the sensors facing up into the current. The design was abandoned, however, because the frame itself would corrupt the flow measurements where orbital wave motions would reverse the horizontal flow in each wave cycle.

Knowing the size, shape, and location of the footprint (**Figure 1**) is not necessary for calculating the O_2 flux from Equation 3, but for an ecological interpretation of the flux and what drives it, this information is warranted. Through modeling, Berg et al. (2007) showed that the footprint for widely used deployment parameters has a long oval shape and typically covers an area of 10– 100 m^2 upstream from the AEC system (**Figure 1**), that the footprint gets larger with increasing measuring height, and that a greater hydraulic roughness results in a smaller footprint. The study also showed that the footprint size for typically encountered environmental conditions is not affected by the magnitude of the current (Berg et al. 2007). Another modeling study showed that due to the size of the footprint, AEC integrates well over typical sediment surface patchiness (Rheuban & Berg 2013). An in situ study in a seagrass meadow by Berger et al. (2020) supported this by measuring comparable hourly fluxes with two systems placed side by side without overlapping footprints.

2.4. Data Treatment

Many steps in AEC data processing have been adapted from standard protocols used in atmospheric flux studies (Aubinet et al. 2012, Burba 2013, Lee et al. 2004). These steps include detrending, which refers to the definition of the \bar{w} and \bar{C} used to calculate w' and C' (Figure 1). Two common approaches are linear detrending, where linear fits to w and C, typically for 15-min time intervals, are used to define \bar{w} and \bar{C} (Berg et al. 2009, Glud et al. 2016, Huettel et al. 2020), and dynamic filtering, where \bar{w} and \bar{C} are defined, for example, as running means (Attard et al. 2020, Berg et al. 2013, Lorrai et al. 2010) or through a low-frequency filter (McCann-Grosvenor et al. 2014, Reimers et al. 2012). Another adapted data-processing step is coordinate rotation of the measured three-dimensional velocity field to ensure that the vertical mean velocity, \bar{w} , equals zero, as assumed in Equation 3 (Lorrai et al. 2010), or is minimized if a large amount of data is available for given flow directions (Lorke et al. 2013). Sometimes a time lag correction is applied

to remove the small, but always present, temporal misalignment between the measured velocity and O_2 data by repeating the flux calculation while shifting the O_2 data in time until the numerically largest flux is found (Attard et al. 2014, Berg et al. 2016, McGinnis et al. 2008). Finally, substrates such as seagrass meadows require relatively large measuring heights to ensure that data are recorded above the canopy. Because seagrass beds also often drive large diurnal variations in the water column O_2 concentration, a storage correction for the change in O_2 stored between the sediment surface and the measuring point can improve the flux extraction (Rheuban et al. 2014a).

A few field conditions are unique to aquatic applications of the eddy covariance technique. including the presence of oscillatory motions generated by surface waves, and may require more elaborate processing. For example, the traditional time lag corrections described above should not be used in the presence of short-period waves and little current, as doing so can result in substantial flux biases (Berg et al. 2015, Volaric et al. 2018). Alternative time lag corrections have been developed for such conditions that rely on aligning the wave signal in the O_2 concentration with the wave signal in the velocity data, but they are not trivial to apply (Berg et al. 2015, Reimers et al. 2016a). By examining different substrates (seagrasses, coral reefs, and sands), Long (2021) found small so-called wave biases (Trowbridge 1998) of up to 4% for O2 fluxes and recommended using larger measuring heights to obtain a spectral gap between current-driven turbulence and wave oscillation frequencies. While this would shift the flux signal toward larger and slower eddies and facilitate removing short-period wave contributions, it could introduce other, possibly larger errors by moving the measuring point away from the surface for which the flux is sought. It would, for example, amplify transient biases from O2 concentration and current velocity changes (Holtappels et al. 2013). As none of these approaches to diminish different kinds of biases associated with waves are universal solutions, more work is needed to improve measurements and flux extractions under this rather common field situation. In that pursuit, it should be recognized that wave motions can contribute to the real total O₂ flux, in addition to the current-driven turbulence, and thus should not be categorically removed from the flux record in ecological studies of benthic substrates (Berg et al. 2015, Long et al. 2015a, Reimers & Fogaren 2021).

Data analysis in the frequency domain—for example, by calculating the cumulative cospectrum of the vertical velocity and O_2 concentration (**Figure 2***f*)—can give additional valuable information on which frequencies are carrying the flux signal and whether a particular O_2 sensor is sufficiently fast to capture it (Berg et al. 2013, Chipman et al. 2012, Reimers et al. 2012).

The AEC technique has been validated in many studies, primarily in comparisons with parallel in situ chamber deployments. Some of these studies are referenced below.

3. KEY FINDINGS FROM DIFFERENT ENVIRONMENTS

AEC studies have produced new quantitative and conceptual knowledge on O_2 dynamics, metabolic rates, and their controls for different benthic substrates. These insights have emerged because AEC includes the full dynamic effects of variable currents, wave action, sediment resuspension, fauna activity, and nutrient and org-C inputs to bottom surfaces. Below, we review some of these findings.

3.1. Cohesive Muddy Sediments

Cohesive, fine-grained muddy sediments (permeability $< 10^{-12} \text{ m}^2$) extend from the coastline to the greatest ocean depths and are globally important for org-C cycling and sequestration. Shallowwater cohesive sediments may exhibit diel cycles of benthic primary production and respiration. In deeper settings, respiration dominates, and it is widely accepted that to avoid artifacts, benthic O_2 fluxes should be measured in situ (Glud et al. 1994, Reimers et al. 1986). The existing database

of in situ measurements with traditional flux methods reveals that benthic O_2 consumption diminishes by two orders of magnitude with depth, from approximately -20 to -40 mmol m⁻² d⁻¹ in coastal waters to approximately -0.2 to -0.4 mmol m⁻² d⁻¹ at abyssal depths (Glud 2008). AEC measurements confirm that trend. For example, at water depths of 22, 65, 300, 1,450, and 2,500 m, the O_2 uptake has been measured at -23, -13, -3.6, -1.6, and -0.9 mmol m⁻² d⁻¹, respectively (Amo-Seco et al. 2021, Glud et al. 2016, Cathalot et al. 2015, Berg et al. 2009, and Donis et al. 2016, respectively).

In situ chambers are perceived as giving accurate flux measurements in cohesive muds with low macrofauna densities. For that reason, they were used to validate the AEC technique for O_2 flux measurements when it was first developed. Deployments of both approaches in two nearshore sediments gave ratios of 0.72 and 0.87 between chamber and AEC fluxes (Berg et al. 2003). Other comparative studies gave a ratio of 1.02 for deep-ocean muddy sediment (Berg et al. 2009) and a ratio of 0.88 for a 65-m-deep sedimentary basin (Glud et al. 2016). A study in estuarine mud resulted in an AEC flux of -31 mmol m⁻² d⁻¹, while parallel deployments of a large chamber (diameter of 80 cm) gave a flux of -40 mmol m⁻² d⁻¹ (Amo-Seco et al. 2021). Bottle incubations of water sampled inside the chamber revealed a significant respiration of -10 mmol m⁻² d⁻¹ and suggested that the difference was driven by a fluff layer that was resuspended when the chamber was installed.

A common perception is that aphotic muddy sediments exhibit only small dynamic changes in O_2 uptake compared with other benthic substrates. AEC measurements have shown that this is not true, and we here give examples of physical, chemical, and biological processes that can give rise to highly dynamic fluxes—processes that are important to appreciate if we are to understand the biogeochemical function of cohesive muds.

Current- and wave-driven motions in the bottom water compress diffusive boundary layers atop intact cohesive sediment surfaces and reduce the total resistance to diffusive O_2 transport into the sediment (Glud et al. 2007, Jørgensen & Des Marais 1990). This reduction is typically substantial in nearshore sediments with high metabolic activity and small O_2 penetration depths (<1–2 mm) and can temporarily stimulate the benthic O_2 flux significantly. Combining AEC fluxes and O_2 microprofiles measured in a sedimentary basin, Glud et al. (2016) estimated that alterations of the diffusive boundary layer by current flow could explain up to 30% of the measured variation in O_2 uptake (**Figure 3***b*).

Fauna activity and behavior are controlled by environmental conditions, and fauna often have distinct tidal and circadian variations in activity level and feeding mode (Naylor 1996, Tessmar-Raible et al. 2011, Wenzhofer & Glud 2004). The effects of these processes were reflected in enhanced rates of benthic O₂ uptake documented using AEC by Glud et al. (2016), who also showed how periods of enhanced tidally driven flow and the resulting elevated near-bed particle density coincided with higher irrigation and filtration activity by brittle stars (**Figure 3***b*). Vacated burrow structures ventilated with bottom water by pressure differences arising from current flow, wave action, and bottom-water density changes can similarly stimulate O₂ uptake in two major ways: by elevating O₂ levels in and around burrow structures and by oxidizing reduced compounds from burrow interiors (Huettel & Gust 1992, Munksby et al. 2002, Ray & Aller 1985). AEC measurements do integrate these effects, but no study has yet investigated how these processes contribute individually to the total flux.

The deep ocean (>200 m) covers 64% of Earth and is vastly underexplored. Despite its relatively low mineralization rates, the vast abyssal plains contribute significantly to the global benthic mineralization (Glud 2008, Stratmann et al. 2019). To date, only a few AEC studies have focused on deep-ocean settings. At a 1,450-m-deep site with fine-grained, fauna-poor mud in Sagami Bay, Japan, Berg et al. (2009) measured AEC O₂ fluxes that averaged -1.6 mmol m⁻² d⁻¹. Parallel



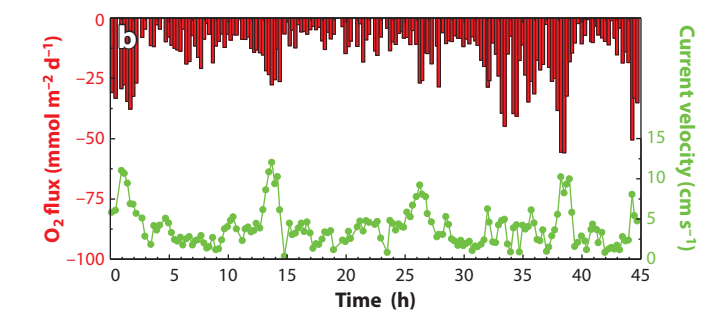


Figure 3

(a) In situ image (approximately 13×19 cm) of a muddy sediment at 65-m depth with a dense population of brittle stars (*Amphiura filiformis*, $\sim 1,100 \text{ m}^{-2}$). Arms of the brittle stars are extending up from the surface. (b) AEC-measured O_2 uptake derived for 15-min time intervals and corresponding current velocity. The data yielded an average O_2 uptake of $-15.0 \text{ mmol m}^{-2} \text{ d}^{-1}$ and a mean current velocity of 3.9 cm s^{-1} . The strong relationship between the O_2 flux and current velocity was caused by alterations of the diffusive boundary-layer thickness, the elevated near-bed particle density enhancing the irrigation and filtration activity of the brittle stars, and the stars' increased respiration. Abbreviation: AEC, aquatic eddy covariance. Panel b adapted from Glud et al. (2016).

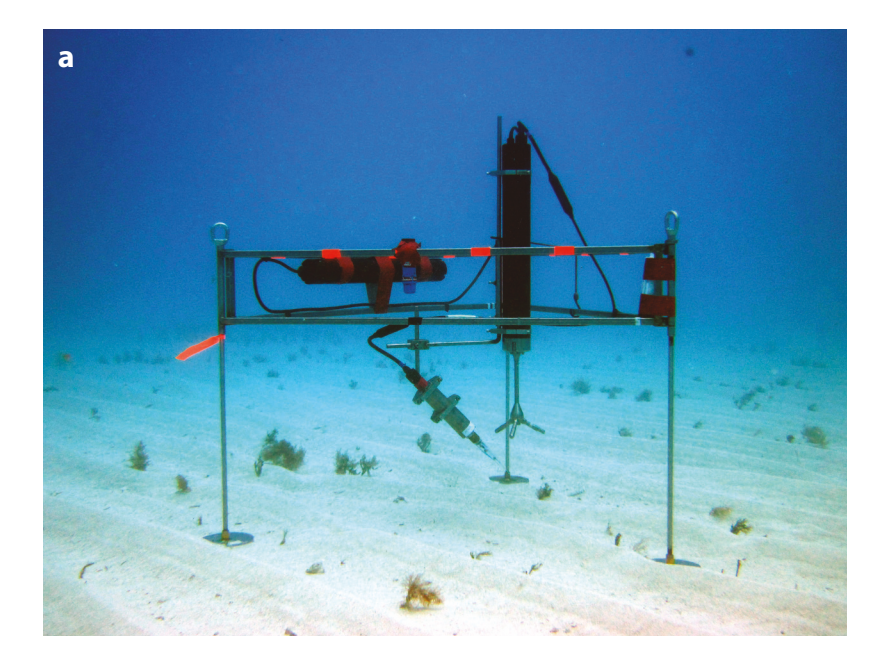
in situ chamber deployments and O_2 microprofile interpretations gave comparable results within 12%. Another comparison at 2,500-m depth in the oligotrophic Fram Strait gave a mean O_2 flux of -0.9 mmol m⁻² d⁻¹ and similarly good agreement among the three approaches (Donis et al. 2016). These studies demonstrate that the benthic metabolic activity and near-bed turbulence levels, even at considerable depths and at low current velocities (in the range of 1–3 cm s⁻¹), are sufficient to enable reliable AEC flux measurements with standard commercially available instrumentation. The study by Donis et al. (2016) represents the deepest AEC measurements to date, although commercial instrumentation is available for depths down to 4,000 m.

The ability of flow to stimulate benthic O₂ uptake by cohesive aphotic sediments via different mechanisms has been in focus in this section, partly because chamber approaches exclude natural bottom-water hydrodynamics. It is, however, important to appreciate that such flow effects are temporary by nature and that, when integrated over long timescales, O₂ uptake by sediment closely reflects its input of reactive org-C. Sustained flow-driven increases in O₂ uptake can only occur if elevated flow also enhances org-C inputs to the sediment. Consequently, flow stimulations of the O₂ uptake for intact cohesive sediments should in most cases be seen as temporary non-steady-state situations manifested over various timescales. AEC measurements should thus be employed over long periods (e.g., days or weeks) when seeking to determine representative average fluxes under in situ conditions (Attard et al. 2016, Berg et al. 2003, Glud et al. 2016). As shown below, this observation applies equally to other substrates as well.

3.2. Permeable Sediments

Permeable sediments (permeability $> 10^{-12}$ m²; Huettel et al. 2014) are found globally along shorelines and on continental shelves and consist largely of silicates in cold and temperate waters and carbonates in tropical settings (Dagg et al. 2004, Eyre et al. 2018). Although they cover less than 10% of the ocean floor, shelf sediments receive approximately 40% of the global benthic org-C input (Muller-Karger et al. 2005). Of this, a large fraction is mineralized in the permeable sediments and thus accounts for a major part of the global benthic org-C cycling (Huettel et al. 2014).

Permeable sediments allow various forms of advective exchange with the water column (**Figure 4**). Deflection of the currents and orbital wave motions by ripples and other topographical



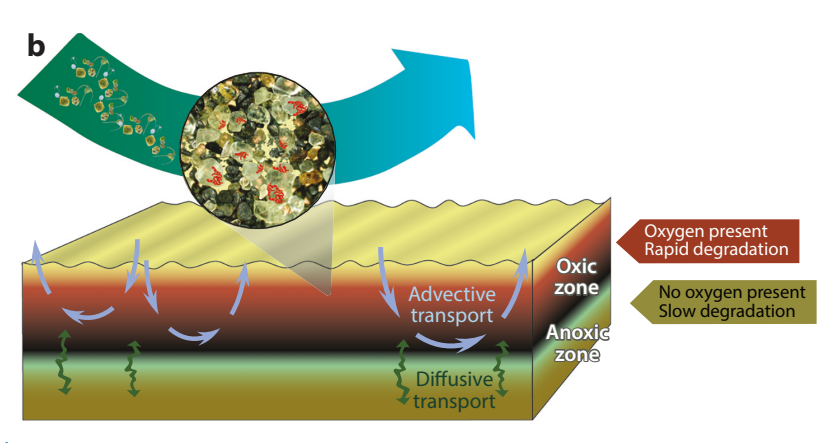


Figure 4

(a) An AEC system deployed at 10-m water depth over rippled, permeable carbonate sand. (b) The stimulation of carbon cycling via filtration of O₂-rich water and organic carbon through the surface layers of permeable sand, which enhances both aerobic microbial mineralization and reoxidation of reduced compounds formed by anaerobic decay. The top sand thus resembles an effective catalytic matrix. These complex processes are difficult to mimic in enclosure approaches for all naturally occurring intensities of current flow and wave action. Abbreviation: AEC, aquatic eddy covariance.

features can drive O₂ and other solutes deep into a permeable sediment (Packman & Brooks 2001, Precht et al. 2004, Thibodeaux & Boyle 1987) and at the same time filter out particulate matter, including org-C (Rusch & Huettel 2000, Rusch et al. 2000, Preziosi-Ribero et al. 2020). This creates an effective catalytic matrix for rapid and sustainably enhanced org-C mineralization while also stimulating reoxidation of reduced compounds formed by anaerobic decay. Permeable sediments, including sandy tidal flats, can host dense faunal communities, creating sediment mounds,

depressions, and three-dimensional burrow structures that, when flushed, enhance exchange with the water column (Meysman et al. 2006). Some permeable sediments are also home to ground-water seepage that can supply nutrients and reduced compounds to benthic surface layers (Moore & Wilson 2005, Moore et al. 2008). These complex mechanisms and feedbacks involving permeable sediments are reflected in their O₂ fluxes, which are often more dynamic and substantial than those of cohesive sediments. O₂ fluxes in permeable sediments are thus best measured by AEC to include effects of all driving environmental variables (Berg et al. 2013, Huettel et al. 2014, Reimers et al. 2012).

Early proof-of-concept tests of AEC for O_2 flux measurements revealed the magnitude of the catalytic effects of permeable sediments by showing a substantial and sustained O_2 uptake of -210 mmol m⁻² d⁻¹ for a sandy riverbed, which was five times as large as fluxes measured at two hypereutrophic estuaries with cohesive muds (Berg et al. 2003). Later, Kuwae et al. (2006) measured nighttime O_2 fluxes of up to -350 mmol m⁻² d⁻¹ over an intertidal sand flat. A detailed AEC study, including 13 field campaigns, at a shallow-water subtropical site in the Gulf of Mexico with coarse silicate sand (permeability $\sim 40 \times 10^{-12}$ m²) gave an annual average nighttime uptake of -191 mmol m⁻² d⁻¹ (Chipman et al. 2016). In addition, Huettel et al. (2020) reported substantial average daytime and nighttime O_2 fluxes of 96 and -84 mmol m⁻² d⁻¹, respectively, for a subtropical ~ 10 -m-deep oligotrophic reef sand in the Florida Keys. These results illustrate that permeable sediments can be highly active sites for both primary production and mineralization processes.

Advection chambers, which have adjustable flow settings to mimic the natural pore-water exchange for permeable sediments (Janssen et al. 2005a,b), have been compared with parallel AEC deployments a number of times. For a shallow-water sand (permeability $\sim 17 \times 10^{-12} \text{ m}^2$), Attard et al. (2015) found agreement between the nighttime O2 fluxes measured by the two approaches with ratios of 0.9-1.3. Another comparison, performed in the Florida Keys over permeable carbonate sand (permeability $\sim 30 \times 10^{-12}$ m²), showed statistically, with one exception, the same fluxes from the two approaches for multiple daytime and nighttime measurements (Huettel et al. 2020). These studies were done under low- to moderate-flow conditions; diverging results were found under more energetic flows forced by strong currents and waves. For example, Berg et al. (2015) measured a nighttime uptake of O_2 by a shallow-water permeable sand (permeability $\sim 13 \times$ 10⁻¹² m²) exposed to current- and wind-driven waves that was 1.9 times larger when quantified by AEC than it was when measured in advection chambers. An extreme difference between the two approaches equaling a factor of 4.1 was found for a highly permeable riverbed composed of sand and gravel (permeability $\sim 230 \times 10^{-12}$ m²) and exposed to a strong flow of 31 cm s⁻¹. Large ocean swells, producing strong, water-depth-dependent oscillatory velocities over Oregon shelf sands (permeability $\sim 30 \times 10^{-12}$ m²), have similarly been documented to elevate AEC O₂ fluxes (Reimers & Fogaren 2021, Reimers et al. 2016b). These comparative studies indicate that AEC measurements may be the only approach that yields uncompromised fluxes in permeable substrates under the naturally occurring wide range of current flows and wave action.

To document the dynamic nature of O_2 fluxes for permeable sediments under natural in situ conditions, Berg et al. (2013) determined relationships between flow velocities and AEC O_2 fluxes for coastal permeable sand (permeability $\sim 18 \times 10^{-12}$ m²) exposed to a repetitive tidally driven current. Regression analysis revealed that an increase in tidal current velocity from ~ 0 to 20 cm s⁻¹ gave an almost fourfold increase in O_2 uptake after short-lived transient effects were removed by averaging. This study additionally documented a tight advective coupling between the water column and the upper sand layer using O_2 fiber optodes buried 1 cm below the surface. Anoxic conditions were measured in the sand at slack tide, while $\sim 65\%$ of the water column O_2 concentration was recorded at ebb and flood. Such short-term increases in O_2 penetration alone translated to an interim sediment O_2 uptake of up to -50 mmol m⁻² d⁻¹ (Berg et al. 2013).

Other AEC studies of permeable sediments, including shallow-water coarse silicate sands (Chipman et al. 2016), have shown similar profound relationships between O₂ uptake and flow. In addition to reflecting an immediate enhanced aerobic org-C respiration, these relationships include other mechanisms, such as aerobic reoxidation of reduced compounds (e.g., Fe⁺, H₂S, and Mn²⁺) from earlier anaerobic org-C respiration, replacement of anoxic pore water with oxic water column water as O₂ penetration increases, and likely immediate respiration of flow-induced, highly labile dissolved and particulate org-C. As discussed above, some of these mechanisms can also affect cohesive sediments, but they are more pronounced for permeable sediments because they allow various forms of advective exchange with the water column. As a result, flow-enhanced flushing of the upper layer of a permeable sediment (**Figure 4**) will increase the supply of highly labile dissolved org-C and filter out or trap particulate org-C, thus supporting sustained elevated O₂ uptake.

The net effect of all these mechanisms was illustrated convincingly in an AEC study of a homogeneous sand at 74 m in the North Sea by McGinnis et al. (2014). Specifically, a 45-h-long data record showed periodic fluctuations in O_2 uptake between ~ 0 and -25 mmol m⁻² d⁻¹ that were closely driven by a repetitive, near-perfect sinusoidal oscillation in tidal flow. Thus, as for cohesive sediments, representative mean values for O_2 uptake by permeable sediments must rely on measurements integrated over a long period of time; in this case, a full tidal cycle is the bare minimum.

3.3. Dense Phototrophic Substrates

Benthic primary producers range from microscopic algae and bacteria to towering kelp and constitute a large proportion of ocean photosynthetic biomass (Smith 1981). Although they can persist under extremely low light levels, down to water depths of hundreds of meters, dense phototrophic habitats such as seagrass meadows and macroalgal canopies are largely restricted to shallower settings (<40 m) (Gattuso et al. 2006). Whole-system O_2 fluxes and derived daily metabolic rates of respiration (R), gross primary production (GPP), and net ecosystem metabolism (NEM) are cornerstone variables when evaluating the health of shallow-water phototrophic ecosystems, trophic status, and contribution to blue C retention. Reliable O_2 fluxes are key for estimating these parameters.

3.3.1. Seagrass meadows. Seagrass meadows are found on all continents except Antarctica, and although they only cover a minute fraction of the ocean floor, they are estimated to account for 10–18% of the global oceanic org-C burial (Fourqurean et al. 2012). Even in comparison with other shallow-water ecosystems, seagrasses are metabolic hot spots, often with manyfold-higher metabolic rates, as documented by parallel AEC measurements over dense seagrass beds and adjacent substrates. During peak seagrass growing season, Hume et al. (2011) and Rheuban et al. (2014a) found by integrating hourly O₂ fluxes for many consecutive days that R and GPP were approximately 10–25 times higher for a temperate *Zostera marina* meadow than for adjacent bare sediment. Koopmans et al. (2020) reported comparable differences between a subtropical *Posidonia oceanica* meadow and nearby bare sand. O₂ fluxes from these studies ranged from approximately –300 mmol m⁻² d⁻¹ at night to 600 mmol m⁻² d⁻¹ during the day for the temperate meadow and from approximately –100 to 250 mmol m⁻² d⁻¹ for the subtropical site.

During daytime, available light [photosynthetically active radiation (PAR)] at a seagrass canopy exerts major control on the size and direction of the O_2 flux, and the temporal response to changes in PAR—for example, caused by drifting clouds—is immediate on the 15-min timescale resolvable by AEC (Long et al. 2015b, Rheuban et al. 2014b). Also, photosynthesis–irradiance curves

generated from AEC data represent the natural whole-ecosystem response to light, integrated horizontally over many plants and vertically through the entire canopy, and often show different trends. For example, in coastal bays in Virginia, Rheuban et al. (2014a) found a young (5 years old) restored seagrass meadow to be light saturated, whereas an older (11 years old), denser adjacent meadow showed no signs of light saturation. This lack of light saturation in dense seagrass meadows can likely be ascribed to self-shading preventing the lower canopy from reaching its maximum photosynthetic production (Binzer et al. 2006, Short 1980).

AEC studies have repeatedly found that current velocity stimulates seagrass meadow respiration at night two- to fourfold for velocity increases in the range of 5–10 cm s⁻¹ (Hume et al. 2011, Long et al. 2015b, Rheuban et al. 2014b). Even though daytime stimulation of respiration and photosynthetic production may counteract one another with respect to the resulting O₂ flux, a study by Hume et al. (2011) indicated that current velocity has a positive effect on production as well. These dependencies during both day and night are likely attributable to several factors, including compression of diffusive boundary layers on seagrass leaves through which gas exchange occurs (Fonseca & Kenworthy 1987, Koch 1994).

Tidal currents and wave action can affect sedimentation and resuspension in seagrass beds (Hansen & Reidenbach 2012) and have a profound impact on benthic O_2 fluxes. For a Z. marina meadow underlain by sandy silt, a fivefold increase in O_2 uptake was measured by AEC during enhanced wave action. Supplemental laboratory experiments with sediment from the site attributed this increase to enhanced oxidation of reduced compounds exposed at the sediment surface and to mineralization of particulate org-C brought into suspension (Camillini et al. 2021). After such events, as calmer weather returned, the O_2 uptake amounted to only $\sim 30\%$ of what it was before.

Laboratory and mesocosm CO₂ enrichment studies have shown equivocal results with respect to stimulation of seagrass production (Borum et al. 2016, Collier et al. 2018, Palacios & Zimmerman 2007). In a field study, Berg et al. (2019) examined this relationship during the peak growing season of a dense *Z. marina* meadow by combining AEC measurements and water column recordings of CO₂ and O₂. The study also included elevated O₂ levels because they can inhibit photosynthesis (Buapet et al. 2013, Mass et al. 2010, Raven & Larkum 2007). The 4.5-fold variation in water column *p*CO₂, the 2.2-fold variation in O₂ concentration, and the concurrent daytime O₂ fluxes did not show any sign of seagrass photosynthesis being stimulated at high CO₂ levels or inhibited at high O₂ levels (Berg et al. 2019). These results were obtained even though CO₂ levels reached those used in the IPCC's 2013 ocean acidification scenarios, and thus do not support the notion that seagrass will be winners in future more acidic oceans with elevated CO₂ concentrations and more frequent temperature extremes.

The largest database of hourly AEC O₂ fluxes for a specific seagrass meadow includes numerous deployments distributed throughout the year and covers 115 full diel cycles for a restored Z. marina meadow on the eastern shore of Virginia (Berger et al. 2020). Pairs of daily R and GPP extracted from this record fall remarkably close to the 1:1 line (**Figure 5b**) and reflect a phototropic system that has rapid internal org-C cycling and is in overall metabolic balance, despite some day-to-day variability between autotrophy and heterotrophy.

Another surprising trend in this long-term record is the variability in paired daily R and GPP on a short timescale. For example, during the month of June (**Figure 5**c), this variability is almost as pronounced as it is for the entire year (**Figure 5**b). This result, obtained under naturally varying in situ conditions, raises issues with the view that benthic metabolism for phototrophic systems follows a somewhat smooth seasonal pattern. In fact, just a few cloudy, poor-weather summer days can reduce seagrass metabolism to below the winter average value (Berger et al. 2020). The highly dynamic nature of seagrass metabolism emphasizes the importance of relying on numerous daylong measurements to correctly determine the trophic status of a seagrass meadow.

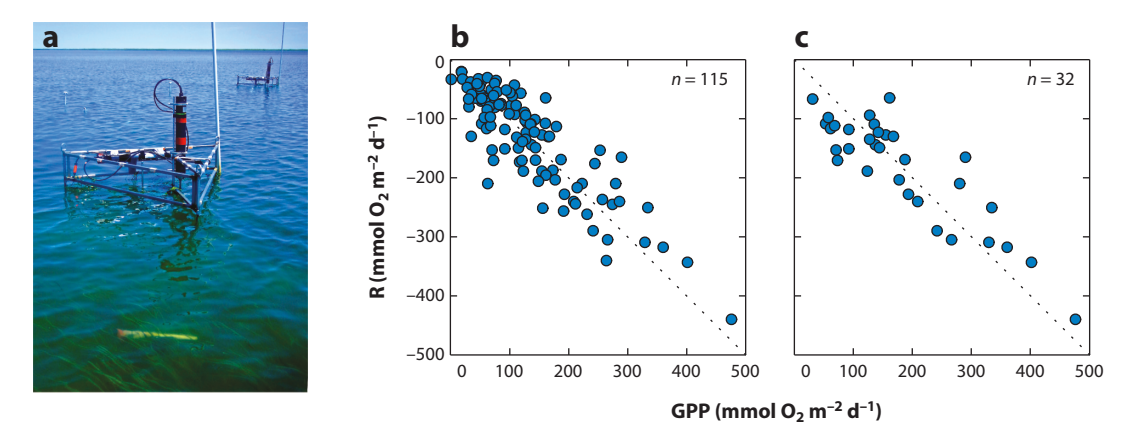


Figure 5

(a) Two AEC systems at low tide deployed \sim 10 m apart over a dense seagrass meadow without overlapping footprint. (b) Daily R versus GPP values, which are distributed close to a 1:1 line (dotted line). The values cover all seasons. (c) Daily R versus GPP values for June, which exhibited almost the same manyfold variations as seen in the full record. Abbreviations: AEC, aquatic eddy covariance; GPP, gross primary production; R, respiration. Panels b and c adapted from Berger et al. (2020).

3.3.2. Fucoid canopies. Macroalgal canopies are often found on rocky shores, where org-C burial is negligible. As a result, they export a large proportion of their net primary production to nourish surrounding habitats, and studies have suggested that a fraction of their production is sequestered in deeper waters and represents a sink of atmospheric CO₂ (Duarte & Cebrian 1996, Krause-Jensen & Duarte 2016).

An AEC study performed through different seasons in the Baltic Sea over the brown alga *Fucus vesiculosus* documented substantial daily NEM values of up to 166 mmol m⁻² d⁻¹ (Attard et al. 2019). It also estimated via a simple regression model that the canopy was autotrophic for two-thirds of the year and highly autotrophic (NEM > 100 mmol m⁻² d⁻¹) for 150 days.

F. vesiculosus has numerous vesicles (air bladders) that provide buoyancy, facilitate spore dispersal, and accumulate considerable amounts of O_2 when exposed to light (Sorrell & Dromgoole 1986). Attard et al. (2019) showed that positive O_2 fluxes measured repeatedly by AEC from a dense F. vesiculosus canopy up into the water column after dusk were likely related to an O_2 release from these vesicles. Additional light and dark microsensor measurements of O_2 stored inside the vesicles supported this explanation.

3.3.3. Invasive *Gracilaria vermiculophylla* on intertidal flats. Native to Japan, the macroalga *Gracilaria vermiculophylla* has invaded coastal waters in the United States and Europe (Gulbransen et al. 2012, Thomsen et al. 2006). Because the alga often colonizes previously bare tidal flats and forms dense canopies, it typically represents a substrate with enhanced org-C cycling. Specifically, night- and daytime O_2 fluxes for a relatively dense *G. vermiculophylla* mat (\sim 60% areal cover) measured by AEC averaged -178 and 139 mmol m⁻² d⁻¹, respectively (Volaric et al. 2019). For reference, an adjacent site with low alga density (\sim 5% areal cover) had negative O_2 fluxes (uptake) during both night and day, with averages of -50 and -25 mmol m⁻² d⁻¹, respectively. The denser mat was submerged only \sim 75% of the time, prohibiting typical estimations of daily R, GPP, and NEM. However, by combining succeeding deployments, Volaric et al. (2019) were able to construct a composite of 24 hourly O_2 fluxes during summer peak algal coverage. These AEC fluxes compared surprisingly well with independent chamber flux measurements of emergent

G. vermiculophylla mats (Davoult et al. 2017) and thus allowed a first-order estimate of daily R, GPP, and NEM values of -178, 169, and -9 mmol m⁻² d⁻¹, respectively (Volaric et al. 2019).

3.4. Hard Substrates

Hard substrates have been well described from a community ecological perspective but are particularly challenging habitats for metabolic studies. Uneven hard surfaces combined with dense and often diverse populations of plants and animals can prohibit traditional flux studies. AEC may be the best or only option in such settings (Berg et al. 2017).

3.4.1. Coral reefs. Coral reefs are among the most complex and diverse ecosystems in the ocean. Their extreme surface rugosity increases the areas where biogeochemical processes may occur, including photosynthesis; per square meter of horizontally projected area, this makes them metabolic supersites.

The first AEC study of shallow-water coral reefs in the Florida Keys found record-high metabolic activities, with average midday O_2 releases approaching 2,000 mmol m⁻² d⁻¹ and night-time uptake near -1,000 mmol m⁻² d⁻¹ (Long et al. 2013). Integrated over many diel cycles, these subtropical summer fluxes gave R, GPP, and NEM values of -570, 940, and 380 mmol m⁻² d⁻¹, respectively, reflecting strong autotrophic conditions. By combining published ex situ coral production rates with in situ AEC fluxes, Long et al. (2013) estimated to the first order that the active O_2 -producing reef surface was at least seven times larger than the projected planar area—a result that explains why no clear light inhibition was seen at PAR levels near 2,000 μ mol m⁻² s⁻¹. Also, likely affected by the uneven and porous structure of the reefs, nighttime respiration doubled when the current velocity increased from approximately 2 to 15 cm s⁻¹ (Long et al. 2013).

Cold-water coral reefs, found globally in deeper aphotic waters, have manyfold-lower metabolic activity levels than their shallow-water tropical counterparts, yet their metabolism is still several factors higher than that of adjacent bare sediments. This pattern was found in three studies that relied on deep-sea landers and remotely operated vehicles to access reefs in North Atlantic waters at depths ranging from 130 to 750 m (Cathalot et al. 2015, de Froe et al. 2019, Rovelli et al. 2015). Methodological challenges working at these depths limited the deployment times in some of these studies and may explain the large range in measured O_2 fluxes, from -12 to -260 mmol m⁻² d⁻¹. Given the substantial variation in O_2 fluxes found by AEC for other benthic substrates under naturally varying in situ conditions, it is not surprising that cold-water coral reefs exhibit similar kinds of dynamics, emphasizing again that long deployment times are needed to obtain representative mean values.

3.4.2. Mussel reefs. Mussel filtration activity is affected by diel and lunar cycles as well as short-term and seasonal changes in temperature, salinity, bottom-water turbulence, and phytoplankton concentration (Kittner & Riisgård 2005, Riisgård et al. 2013). This reinforces, as in other benthic environments, that the full picture of mussel reef biotic functioning must be obtained under in situ conditions and by approaches that integrate these many relationships.

In an AEC study covering different seasons at a 5-m-deep Mytilus trossulus reef in the Baltic Sea with an impressive mussel density of \sim 50,000 m⁻², Attard et al. (2020) measured midday O_2 releases of up to 450 mmol m⁻² d⁻¹ and nighttime uptakes of similar magnitude. When integrated over days within seasons, these O_2 fluxes gave mean R values between -64 and -112 mmol m⁻² d⁻¹ and GPP values between 5 and 70 mmol m⁻² d⁻¹, indicating strong heterotrophic conditions and underlining the important roles of mussel filtration in supplying org-C to the reef.

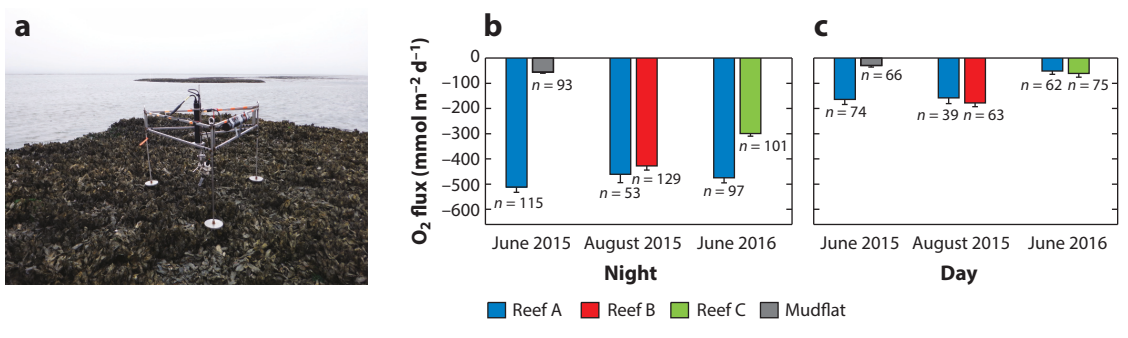


Figure 6

(a) An AEC system deployed on an intertidal *Crassostrea virginica* oyster reef. (b) Nighttime O_2 uptake for three reefs with different oyster densities (244, 175, and 106 m⁻² for reefs A, B, and C, respectively) and an adjacent mudflat. (c) Daytime O_2 uptake for the same reefs and mudflat. The uptake was reduced substantially relative to the nighttime uptake because of photosynthetic production. Abbreviation: AEC, aquatic eddy covariance. Panels b and c adapted with permission from Volaric et al. (2018).

3.4.3. Intertidal oyster reefs. Over the last century, oyster reefs have been globally depleted by ~85% (Beck et al. 2011), mainly due to overharvesting (Jackson et al. 2001) and disease (Oliver et al. 1998). This has triggered substantial restoration efforts in North America and Europe and more focus on defining new ways to assess their health—for example, by using AEC measurements (Reidenbach et al. 2013; Volaric et al. 2018, 2020).

Extensive summer AEC measurements over intertidal *Crassostrea virginica* oyster reefs on the coast of Virginia documented that one natural and two restored reefs had manyfold-higher metabolic activities than those in adjacent bare, muddy sediments (**Figure 6**). Furthermore, these measurements revealed that all reefs were strongly heterotrophic and had surprisingly similar R rates when normalized by density (between -1.8 and -2.3 mmol m⁻² d⁻¹ oyster⁻¹) (Volaric et al. 2018). In a parallel long-term monitoring study covering four years of AEC measurements, Volaric et al. (2020) showed substantial seasonal and interannual variations in oyster reef metabolism, the latter of which included a significant oyster die-off. The seasonal variation amounted to a three-to fourfold-higher summer metabolic activity relative to fall and spring levels, likely related to temperature effects on oyster filtering (Haure et al. 1998, Shumway & Koehn 1982), microalgae abundance, and microbial activity (Apple et al. 2006). A tight relationship between reef metabolism and oyster density for the entire four-year period suggests that AEC measurements may be used to monitor oyster health.

3.4.4. Vertical rock walls and exposed bedrock. At 18-m water depth in a Greenlandic fjord, Glud et al. (2010) deployed an AEC system on an ~80 × 10 m vertical rock surface with high densities of the suspension-feeding sea cucumber *Psolus fabricii*. The average nighttime O₂ uptake of ~29 mmol m⁻² d⁻¹ was surprisingly large, and was comparable to rates measured in the same study at four nearby horizontal benthic substrates (~17 to ~48 mmol m⁻² d⁻¹), including diatom-covered muds and consolidated muddy sand with shell debris. This result, measured during the Arctic spring, suggests that epifauna attached to vertical walls can feed efficiently on pelagic production and scale with horizontal benthic systems. For reference, a parallel seasonal study of a near-horizontal rocky surface in the same fjord with interstices between rocks filled with coarse gravels and relict shells measured average nighttime spring, summer, and fall O₂ fluxes between ~1.9 and ~41 mmol m⁻² d⁻¹ (Attard et al. 2014). These studies show that fairly high metabolic activities can be reached by communities covering rock surfaces, regardless of slope, in cold polar oligotrophic settings.

3.4.5. Sea ice. Submerged sea ice interfaces represent another complex ecosystem where AEC studies have clear advantages. During an early spring period when the ice—water O_2 exchange was dominated by biological processes as opposed to physical freeze—melt processes, Long et al. (2012) measured a nighttime O_2 uptake below 0.7-m-thick sea ice in southwest Greenland of between -1.5 and -2.5 mmol m⁻² d⁻¹. During daytime, at light levels of 12–18 μ mol photons m⁻² s⁻¹ below the sea ice, respiration was counterbalanced by an equally sized photosynthetic ice algal production. The study documented that the algal community was well adapted to minute light levels, as also reflected by indications of light saturation at approximately 4 μ mol photons m⁻² s⁻¹. During times with substantial ice melt, measured AEC O_2 fluxes should be interpreted with caution because they, in addition to biologically mediated exchange, can comprise significant contributions from O_2 -depleted meltwater released over the ice—water interface (Attard et al. 2018, Glud et al. 2014).

4. NEW APPLICATIONS

4.1. Air-Water Gas Exchange

Air—water gas exchange is viewed as the primary source of uncertainty in many common wholesystem metabolic estimates (Raymond & Cole 2001). A new promising application of the AEC technique can reduce this uncertainty and improve quantifications of greenhouse gas exchange over the air—water interface.

By orienting AEC sensors to measure right below the air–water interface, O_2 fluxes across the interface can be determined accurately and with high temporal resolution (Berg & Pace 2017, Berg et al. 2017, Long & Nicholson 2018). Moreover, by combining such air–water O_2 fluxes with concurrently measured bulk O_2 concentrations in the surface water, standard gas exchange coefficients (k_{600}) can be derived and translated into coefficients for any gas of interest (Berg et al. 2020). If concentrations of greenhouse gases such as CO_2 , CH_4 , and N_2O are also measured or calculated for each side of the air–water interface, emissions of these gases can then be determined.

Fast-responding O₂ sensors are inherently sensitive to temperature changes (Gundersen et al. 1998). A sensor placed in a constant molar O₂ concentration will show a signal increase if the temperature increases. Because heat fluxes at the air–water interface are usually substantial compared with those in benthic environments, O₂ sensors used for air–water flux measurements should be corrected using high-speed temperature recordings made at the same point where the O₂ concentrations are measured (Berg & Pace 2017); otherwise, turbulent temperature fluctuations associated with the heat eddy flux will mistakenly be recorded as O₂ fluctuations and bias the O₂ eddy flux calculation. Dual O₂–temperature sensors (Berg et al. 2016) are thus an optimal choice for air–water gas exchange measurements.

Air—water gas exchange can also be measured from a moving platform in near-stagnant waters (Berg et al. 2020). Further evaluations of such mobile measurements under different in situ conditions are needed to fully evaluate this new approach. As a spin-off, mobile measurements may have a future in benthic environments: By mounting AEC sensors on an autonomous underwater vehicle that moves at a controlled speed over a benthic surface, accurate fluxes along transects can likely be measured. Similar flyover measurements have been performed for decades in the atmospheric boundary layer (Crawford et al. 1996).

4.2. Long-Term Ocean Observatory Measurements

As AEC has become established as an approach for measuring benthic O₂ fluxes, so have ocean observing networks providing long-term data records that enhance our knowledge of

fundamental ocean phenomena. Because available AEC hardware is readily hardwired to external power sources and technologies exist to stream data to shore, including AEC measurements in ocean observatories is an achievable goal.

Reimers et al. (2020) demonstrated that such a setup is feasible and determined O_2 and heat fluxes over 222 days at a seafloor observatory at 100-m water depth. If several problems are solved—most notably associated with biofouling and sensor longevity or replacement—then the path will be open toward long-term underwater AEC flux networks.

5. SYNTHESIS AND CONCLUDING REMARKS

During the last two decades, AEC has proven to be a highly versatile noninvasive technique for measuring O_2 fluxes at aquatic interfaces. Most applications have focused on benthic surfaces, but the approach has also been used beneath sea ice and air—water interfaces. AEC studies have produced benthic O_2 fluxes that span more than three orders of magnitude, with end members being subtropical coral reefs and deep, cold abyssal plains. The obtained fluxes have informed us about org-C cycling, ecosystem health, trophic status, and blue C contributions for many aquatic substrates and revealed physical, chemical, and biological drivers of their O_2 exchange. This body of work has additionally demonstrated that quantitative and conceptual knowledge of O_2 exchange dynamics is best obtained from measurements taken in situ, under naturally varying environmental conditions, and, importantly, that representative mean values for a given period must integrate over all timescales that affect the local O_2 exchange within that period.

While some findings reviewed here are substrate specific, others appear to be universal across all aquatic interfaces. The latter include a strong stimulating effect that even moderate current flows have intermittently on O₂ fluxes. For example, sediments (such as aphotic cohesive muds) have been generally viewed as having near-static O₂ exchange rates, at least on short timescales, but AEC measurements have shown that they typically have profound flow-driven O₂ exchange dynamics, even on an hourly timescale. Also, for permeable substrates, such as sands, significant flow effects were predicted years ago by laboratory and model studies, but they have now been confirmed by direct in situ AEC measurements. Strong links between O₂ flux and current flow have, to our knowledge, been found in all AEC measurements substantial enough to allow systematic regression analysis.

Another universal finding is that light-exposed substrates, regardless of what kind of photosynthesizing organism they host, add another complex layer to O_2 flux dynamics. AEC studies have shown repeatedly that light-driven dynamics have multiple timescales—from as short as near-immediate minute-scale responses during days with drifting clouds to as long as weeks. The latter include, for example, highly productive phototrophic substrates that enter a hibernation stage with highly reduced O_2 fluxes, both in the day and at night, during persistent periods with dark, over-cast weather. AEC studies have documented that this pattern can be as pronounced as differences between peak summer and winter fluxes and that, ecologically, it reflects a benthic ecosystem with rapid internal C cycling.

For fauna-populated substrates, AEC measurements have shown a tight coupling between O_2 fluxes and faunal density and activity, the latter of which are often controlled by available food in the bottom water. These patterns have been found consistently for substrates such as fauna-rich muddy sediments, mussel reefs, and intertidal oyster reefs, and they represent another important natural response that is hard to study with other approaches.

We are acutely aware that aquatic environments across the globe are undergoing adverse changes due to factors such as agricultural runoff, land use changes, and, most importantly, greenhouse gas emissions triggering global warming, ocean acidification, and sea level rise. Future AEC studies, along with many other means of noninvasive in situ environmental assessments, can reveal impacts of these drivers and point to remediating measures to mitigate adverse changes.

SUMMARY POINTS

- 1. The aquatic eddy covariance (AEC) technique measures underwater O₂ fluxes without disturbing the natural environment. This is a key advantage, as aquatic O₂ exchange processes are controlled largely by dynamic environmental conditions.
- 2. AEC has a high temporal resolution (\sim 15 min) that captures short-term natural variability and averages over a large surface area (typically 10–100 m²) that integrates across the patchiness typical of aquatic habitats.
- 3. AEC has been used mostly to measure O₂ fluxes between benthic substrates and the water above, but it has also been applied to measure fluxes at submerged vertical cliff walls and below sea ice—water and air—water interfaces. It has been applied from stationary and mobile platforms and integrated in ocean observatories.
- 4. AEC O₂ fluxes have provided novel insights about in situ organic matter cycling, ecosystem health and services, trophic status, and blue carbon contributions for many aquatic substrates.
- 5. AEC measurements have revealed physical, chemical, and biological drivers of O₂ exchange for numerous aquatic substrates. The most important short-term drivers include flow, light, and animal activity.
- 6. AEC measurements have demonstrated that underwater O₂ fluxes are highly dynamic and that representative mean values for a given period must integrate over all timescales that affect the forcing of the O₂ exchange within that period.
- 7. Given its noninvasive nature, the AEC technique is poised for wider use, analogous to the development that occurred in atmospheric boundary-layer research, where the equivalent approach has become the standard method in assessments of land–air fluxes.

DISCLOSURE STATEMENT

The authors are not aware of any affiliations, memberships, funding, or financial holdings that might be perceived as affecting the objectivity of this review.

ACKNOWLEDGMENTS

P.B. was supported by the National Science Foundation (NSF) through grants from the Virginia Coast Reserve Long-Term Ecological Research Program (DEB-1832221) and other NSF grants (OCE-1824144 and OCE-1851424). M.H. and C.E.R. were also supported by NSF grants (OCE-1851290 and OCE-1634319, respectively). R.N.G. and K.M.A. were supported by grants from the European Research Council (669947), Danish National Research Foundation (DNRF145), and Danish National Research Council (FNU7014-00078).

LITERATURE CITED

Amo-Seco M, Castro CG, Villacieros-Robineau N, Alonso-Pérez F, Graña R, et al. 2021. Benthic oxygen fluxes in a coastal upwelling system (Ria de Vigo, NW Iberia) measured by aquatic eddy covariance. Mar. Ecol. Prog. Ser. 670:15–31

- Apple JK, Del Giorgio PA, Kemp WM. 2006. Temperature regulation of bacterial production, respiration, and growth efficiency in a temperate salt-marsh estuary. Aquat. Microb. Ecol. 43:243–54
- Attard KM, Glud RN, McGinnis DF, Rysgaard S. 2014. Seasonal rates of benthic primary production in a Greenland fjord measured by aquatic eddy correlation. *Limnol. Oceanogr.* 59:1555–69
- Attard KM, Hancke K, Sejr MK, Glud RN. 2016. Benthic primary production and mineralization in a High Arctic fjord: in situ assessments by aquatic eddy covariance. *Mar. Ecol. Prog. Ser.* 554:35–50
- Attard KM, Rodil IF, Berg P, Mogg AO, Westerbom M, et al. 2020. Metabolism of a subtidal rocky mussel reef in a high-temperate setting: pathways of organic C flow. *Mar. Ecol. Prog. Ser.* 645:41–54
- Attard KM, Rodil IF, Berg P, Norkko J, Norkko A, Glud RN. 2019. Seasonal metabolism and carbon export potential of a key coastal habitat: the perennial canopy-forming macroalga Fucus vesiculosus. Limnol. Oceanogr. 64:149–64
- Attard KM, Søgaard DH, Piontek J, Lange BA, Katlein C, et al. 2018. Oxygen fluxes beneath Arctic land-fast ice and pack ice: towards estimates of ice productivity. *Polar Biol*. 41:2119–34
- Attard KM, Stahl H, Kamenos NA, Turner G, Burdett HL, Glud RN. 2015. Benthic oxygen exchange in a live coralline algal bed and an adjacent sandy habitat: an eddy covariance study. Mar. Ecol. Prog. Ser. 535:99–115
- Aubinet M, Vesala T, Papale D. 2012. Eddy Covariance: A Practical Guide to Measurement and Data Analysis.

 Dordrecht, Neth.: Springer
- Baldocchi DD. 2003. Assessing the eddy covariance technique for evaluating carbon dioxide exchange rates of ecosystems: past, present and future. Glob. Change Biol. 9:479–92
- Baldocchi DD. 2013. A brief history on eddy covariance flux measurements: a personal perspective. FluxLetter, March, pp. 1–8
- Beck MW, Brumbaugh RD, Airoldi L, Carranza A, Coen LD, et al. 2011. Oyster reefs at risk and recommendations for conservation, restoration, and management. *BioScience* 61:107–16
- Berg P, Delgard ML, Glud RN, Huettel M, Reimers CE, Pace ML. 2017. Non-invasive flux measurements at the benthic interface: the aquatic eddy covariance technique. *Limnol. Oceanogr. e-Lect.* 7:1–50
- Berg P, Delgard ML, Polsenaere P, McGlathery KJ, Doney SC, Berger AC. 2019. Dynamics of benthic metabolism, O₂, and pCO₂ in a temperate seagrass meadow. *Limnol. Oceanogr*: 64:2586–604
- Berg P, Glud RN, Hume A, Stahl H, Oguri K, et al. 2009. Eddy correlation measurements of oxygen uptake in deep ocean sediments. *Limnol. Oceanogr. Methods* 7:576–84
- Berg P, Huettel M. 2008. Monitoring the seafloor using the noninvasive eddy correlation technique: integrated benthic exchange dynamics. *Oceanography* 21(4):164–67
- Berg P, Koopmans D, Huettel M, Li H, Mori K, Wüest A. 2016. A new robust dual oxygen-temperature sensor for aquatic eddy covariance measurements. *Limnol. Oceanogr. Methods* 14:151–67
- Berg P, Long MH, Huettel M, Rheuban JE, McGlathery KJ, et al. 2013. Eddy correlation measurements of oxygen fluxes in permeable sediments exposed to varying current flow and light. *Limnol. Oceanogr*: 58:1329–43
- Berg P, Pace ML. 2017. Continuous measurement of air-water gas exchange by underwater eddy covariance. Biogeosciences 14:5595–606
- Berg P, Pace ML, Buelo CD. 2020. Air-water gas exchange in lakes and reservoirs measured from a moving platform by underwater eddy covariance. *Limnol. Oceanogr. Methods* 18:424–36
- Berg P, Reimers CE, Rosman JH, Huettel M, Delgard ML, et al. 2015. Technical note: time lag corrections of eddy correlation data measured in presence of waves. *Biogeosciences* 12:6721–35
- Berg P, Roy H, Janssen F, Meyer V, Jorgensen BB, et al. 2003. Oxygen uptake by aquatic sediments measured with a novel non-invasive eddy-correlation technique. *Mar. Ecol. Prog. Ser.* 261:75–83
- Berg P, Roy H, Wiberg PL. 2007. Eddy correlation flux measurements: the sediment surface area that contributes to the flux. *Limnol. Oceanogr.* 52:1672–84
- Berger AC, Berg P, McGlathery KJ, Delgard ML. 2020. Long-term trends and resilience of seagrass metabolism: a decadal aquatic eddy covariance study. *Limnol. Oceanogr*: 65:1423–38
- Binzer T, Sand-Jensen K, Middelboe A-L. 2006. Community photosynthesis of aquatic macrophytes. *Limnol. Oceanogr.* 51:2722–33
- Borum J, Pedersen O, Kotula L, Fraser MW, Statton J, et al. 2016. Photosynthetic response to globally increasing CO₂ of co-occurring temperate seagrass species. *Plant Cell Environ*. 39:1240–50

- Buapet P, Rasmusson LM, Gullström M, Björk M. 2013. Photorespiration and carbon limitation determine productivity in temperate seagrasses. *PLOS ONE* 8:e83804
- Burba G. 2013. Eddy Covariance Method for Scientific, Industrial, Agricultural, and Regulatory Applications: A Field Book on Measuring Ecosystem Gas Exchange and Areal Emission Rates. Lincoln, NE: LI-COR Biosci.
- Camillini N, Attard KM, Eyre BD, Glud RN. 2021. Resolving community metabolism of eelgrass Zostera marina meadows by benthic flume-chambers and eddy covariance in dynamic coastal environments. Mar. Ecol. Prog. Ser. 661:67–114
- Canfield DE, Thamdrup B, Hansen JW. 1993. The anaerobic degradation of organic matter in Danish coastal sediments: iron reduction, manganese reduction, and sulfate reduction. Geochim. Cosmochim. Acta 57:3867–83
- Cathalot C, Van Oevelen D, Cox T, Kutti T, Lavaleye M, et al. 2015. Cold-water coral reefs and adjacent sponge grounds: hotspots of benthic respiration and organic carbon cycling in the deep sea. Front. Mar. Sci. 2:37
- Chipman L, Berg P, Huettel M. 2016. Benthic oxygen fluxes measured by eddy covariance in permeable Gulf of Mexico shallow-water sands. Aquat. Geochem. 22:529–54
- Chipman L, Huettel M, Berg P, Meyer V, Klimant I, et al. 2012. Oxygen optodes as fast sensors for eddy correlation measurements in aquatic systems. *Limnol. Oceanogr. Methods* 10:304–16
- Collier CJ, Langlois L, Ow Y, Johansson C, Giammusso M, et al. 2018. Losing a winner: thermal stress and local pressures outweigh the positive effects of ocean acidification for tropical seagrasses. New Phytol. 219:1005–17
- Crawford TL, Dobosy RJ, McMillen RT, Vogel CA, Hicks BB. 1996. Air-surface exchange measurement in heterogeneous regions: extending tower observations with spatial structure observed from small aircraft. Glob. Change Biol. 2:275–85
- Dagg M, Benner R, Lohrenz S, Lawrence D. 2004. Transformation of dissolved and particulate materials on continental shelves influenced by large rivers: plume processes. Cont. Shelf Res. 24:833–58
- Davoult D, Surget G, Stiger-Pouvreau V, Noisette F, Riera P, et al. 2017. Multiple effects of a *Gracilaria* vermiculophylla invasion on estuarine mudflat functioning and diversity. Mar. Environ. Res. 131:227–35
- de Froe E, Rovelli L, Glud RN, Maier SR, Duineveld G, et al. 2019. Benthic oxygen and nitrogen exchange on a cold-water coral reef in the north-east Atlantic Ocean. *Front. Mar. Sci.* 6:665
- Donis D, McGinnis DF, Holtappels M, Felden J, Wenzhoefer F. 2016. Assessing benthic oxygen fluxes in oligotrophic deep sea sediments (HAUSGARTEN observatory). *Deep-Sea Res. I* 111:1–10
- Duarte CM, Cebrian J. 1996. The fate of marine autotrophic production. Limnol. Oceanogr. 41:1758–66
- Eyre BD, Cyronak T, Drupp P, De Carlo EH, Sachs JP, Andersson AJ. 2018. Coral reefs will transition to net dissolving before end of century. Science 359:908–11
- Fonseca MS, Kenworthy WJ. 1987. Effects of current on photosynthesis and distribution of seagrasses. Aquat. Bot. 27:59–78
- Fourqurean JW, Duarte CM, Kennedy H, Marbà N, Holmer M, et al. 2012. Seagrass ecosystems as a globally significant carbon stock. *Nat. Geosci.* 5:505–9
- Gattuso JP, Gentili B, Duarte CM, Kleypas JA, Middelburg JJ, Antoine D. 2006. Light availability in the coastal ocean: impact on the distribution of benthic photosynthetic organisms and their contribution to primary production. *Biogeosciences* 3:489–513
- Glud RN. 2008. Oxygen dynamics of marine sediments. Mar. Biol. Res. 4:243-89
- Glud RN, Berg P, Fossing H, Jorgensen BB. 2007. Effect of the diffusive boundary layer on benthic mineralization and O₂ distribution: a theoretical model analysis. *Limnol. Oceanogr.* 52:547–57
- Glud RN, Berg P, Hume A, Batty P, Blicher ME, et al. 2010. Benthic O₂ exchange across hard-bottom substrates quantified by eddy correlation in a sub-Arctic fjord. *Mar. Ecol. Prog. Ser.* 417:1–12
- Glud RN, Berg P, Stahl H, Hume A, Larsen M, et al. 2016. Benthic carbon mineralization and nutrient turnover in a Scottish sea loch: an integrative in situ study. *Aquat. Geochem.* 22:443–67
- Glud RN, Gundersen JK, Jorgensen BB, Revsbech NP, Schulz HD. 1994. Diffusive and total oxygen uptake of deep-sea sediments in the eastern South Atlantic Ocean: in situ and laboratory measurements. *Deep-Sea Res. I* 41:1767–88
- Glud RN, Rysgaard S, Turner G, McGinnis DF, Leakey RJ. 2014. Biological-and physical-induced oxygen dynamics in melting sea ice of the Fram Strait. *Limnol. Oceanogr.* 59:1097–111

- Gulbransen DJ, McGlathery KJ, Marklund M, Norris JN, Gurgel CFD. 2012. Gracilaria vermiculophylla (Rhodophyta, Gracilarias) in the Virginia coastal bays, USA: cox1 analysis reveals high genetic richness of an introduced macroalga. 7. Phycol. 48:1278–83
- Gundersen JK, Ramsing NB, Glud RN. 1998. Predicting the signal of O₂ microsensors from physical dimensions, temperature, salinity, and O₂ concentration. *Limnol. Oceanogr.* 43:1932–37
- Hansen JC, Reidenbach MA. 2012. Wave and tidally driven flows in eelgrass beds and their effect on sediment suspension. Mar. Ecol. Prog. Ser. 448:271–87
- Haure J, Penisson C, Bougrier S, Baud J. 1998. Influence of temperature on clearance and oxygen consumption rates of the flat oyster *Ostrea edulis*: determination of allometric coefficients. *Aquaculture* 169:211–24
- Hayes FR, Macaulay MA. 1959. Lake water and sediment: V. Oxygen consumed in water over sediment cores. Limnol. Oceanogr. 4:291–98
- Holtappels M, Glud RN, Donis D, Liu B, Hume A, et al. 2013. Effects of transient bottom water currents and oxygen concentrations on benthic exchange rates as assessed by eddy correlation measurements. *J. Geophys. Res. Oceans* 118:1157–69
- Huettel M, Berg P, Kostka JE. 2014. Benthic exchange and biogeochemical cycling in permeable sediments. Annu. Rev. Mar. Sci. 6:29–51
- Huettel M, Berg P, Merikhi A. 2020. Technical note: measurements and data analysis of sediment–water oxygen flux using a new dual-optode eddy covariance instrument. *Biogeosciences* 17:4459–76
- Huettel M, Gust G. 1992. Solute release mechanisms from confined sediment cores in stirred benthic chambers and flume flows. Mar. Ecol. Prog. Ser. 82:187–97
- Hume AC, Berg P, McGlathery KJ. 2011. Dissolved oxygen fluxes and ecosystem metabolism in an eelgrass (*Zostera marina*) meadow measured with the eddy correlation technique. *Limnol. Oceanogr.* 56:86–96
- Jackson JB, Kirby MX, Berger WH, Bjorndal KA, Botsford LW, et al. 2001. Historical overfishing and the recent collapse of coastal ecosystems. Science 293:629–37
- Janssen F, Faerber P, Huettel M, Meyer V, Witte U. 2005a. Pore-water advection and solute fluxes in permeable marine sediments (I): calibration and performance of the novel benthic chamber system Sandy. Limnol. Oceanogr. 50:768–78
- Janssen F, Huettel M, Witte U. 2005b. Pore-water advection and solute fluxes in permeable marine sediments (II): benthic respiration at three sandy sites with different permeabilities (German Bight, North Sea). *Limnol. Oceanogr*: 50:779–92
- Jørgensen BB. 1982. Mineralization of organic matter in the sea bed—the role of sulphate reduction. Nature 296:643–45
- Jørgensen BB, Des Marais DJ. 1990. The diffusive boundary layer of sediments: oxygen microgradients over a microbial mat. Limnol. Oceanogr. 35:1343–55
- Kittner C, Riisgård HU. 2005. Effect of temperature on filtration rate in the mussel *Mytilus edulis*: no evidence for temperature compensation. *Mar. Ecol. Prog. Ser.* 305:147–52
- Koch EW. 1994. Hydrodynamics, diffusion-boundary layers and photosynthesis of the seagrasses *Thalassia testudinum* and *Cymodocea nodosa*. *Mar. Biol.* 118:767–76
- Koopmans D, Holtappels M, Chennu A, Weber M, de Beer D. 2020. High net primary production of Mediterranean seagrass (*Posidonia oceanica*) meadows determined with aquatic eddy covariance. *Front. Mar. Sci.* 7:118
- Krause-Jensen D, Duarte CM. 2016. Substantial role of macroalgae in marine carbon sequestration. Nat. Geosci. 9:737–42
- Kuwae T, Kamio K, Inoue T, Miyoshi E, Uchiyama Y. 2006. Oxygen exchange flux between sediment and water in an intertidal sandflat, measured in situ by the eddy-correlation method. Mar. Ecol. Prog. Ser. 307:59–68
- Lee X, Massman W, Law B. 2004. Handbook of Micrometeorology: A Guide for Surface Flux Measurement and Analysis. Dordrecht, Neth.: Kluwer Acad.
- Long MH. 2021. Aquatic biogeochemical eddy covariance fluxes in the presence of waves. J. Geophys. Res. Oceans 126:e2020JC016637
- Long MH, Berg P, de Beer D, Zieman JC. 2013. In situ coral reef oxygen metabolism: an eddy correlation study. PLOS ONE 8:e58581

- Long MH, Berg P, Falter JL. 2015a. Seagrass metabolism across a productivity gradient using the eddy covariance, Eulerian control volume, and biomass addition techniques. 7. Geophys. Res. Oceans 120:3624–39
- Long MH, Berg P, McGlathery KJ, Zieman JC. 2015b. Sub-tropical seagrass ecosystem metabolism measured by eddy covariance. Mar. Ecol. Prog. Ser. 529:75–90
- Long MH, Charette MA, Martin WR, McCorkle DC. 2015c. Oxygen metabolism and pH in coastal ecosystems: Eddy Covariance Hydrogen ion and Oxygen Exchange System (ECHOES). Limnol. Oceanogr. Methods 13:438–50
- Long MH, Koopmans D, Berg P, Rysgaard S, Glud RN, Søgaard DH. 2012. Oxygen exchange and ice melt measured at the ice-water interface by eddy correlation. Biogeosciences 9:1957–67
- Long MH, Nicholson DP. 2018. Surface gas exchange determined from an aquatic eddy covariance floating platform. Limnol. Oceanogr. Methods 16:145–59
- Lorke A, McGinnis DF, Maeck A. 2013. Eddy-correlation measurements of benthic fluxes under complex flow conditions: effects of coordinate transformations and averaging time scales. *Limnol. Oceanogr. Methods* 11:425–37
- Lorrai C, McGinnis DF, Berg P, Brand A, Wüest A. 2010. Application of oxygen eddy correlation in aquatic systems. J. Atmos. Ocean. Technol. 27:1533–46
- Mass T, Genin A, Shavit U, Grinstein M, Tchernov D. 2010. Flow enhances photosynthesis in marine benthic autotrophs by increasing the efflux of oxygen from the organism to the water. *PNAS* 107:2527–31
- McCann-Grosvenor K, Reimers CE, Sanders RD. 2014. Dynamics of the benthic boundary layer and seafloor contributions to oxygen depletion on the Oregon inner shelf. Cont. Shelf Res. 84:93–106
- McGinnis DF, Berg P, Brand A, Lorrai C, Edmonds TJ, Wüest A. 2008. Measurements of eddy correlation oxygen fluxes in shallow freshwaters: towards routine applications and analysis. Geophys. Res. Lett. 35:L04403
- McGinnis DF, Sommer S, Lorke A, Glud RN, Linke P. 2014. Quantifying tidally driven benthic oxygen exchange across permeable sediments: an aquatic eddy correlation study. *J. Geophys. Res. Oceans* 119:6918–32
- McPhee MG. 1992. Turbulent heat flux in the upper ocean under sea ice. *J. Geophys. Res. Oceans* 97:5365–79 Meysman FJR, Galaktionov ES, Gribsholt B, Middelburg JJ. 2006. Bioirrigation in permeable sediments:
- Moore WS, Sarmiento JL, Key RM. 2008. Submarine groundwater discharge revealed by ²²⁸Ra distribution in the upper Atlantic Ocean. Nat. Geosci. 1:309–11

advective pore-water transport induced by burrow ventilation. Limnol. Oceanogr. 51:142-56

- Moore WS, Wilson AM. 2005. Advective flow through the upper continental shelf driven by storms, buoyancy, and submarine groundwater discharge. *Earth Planet. Sci. Lett.* 235:564–76
- Mortimer CH. 1941. The exchange of dissolved substances between mud and water in lakes. *J. Ecol.* 29:280–329
- Muller-Karger FE, Varela R, Thunell R, Luerssen R, Hu C, Walsh J. 2005. The importance of continental margins in the global carbon cycle. *Geophys. Res. Lett.* 32:L01602
- Munksby N, Benthien M, Glud RN. 2002. Flow-induced flushing of relict tube structures in the central Skagerrak (Norway). *Mar. Biol.* 141:939–45
- Naylor E. 1996. Crab clockwork: the case for interactive circatidal and circadian oscillators controlling rhythmic locomotor activity of Carcinus maenas. Chronobiol. Int. 13:153–61
- Odum HT. 1957. Trophic structure and productivity of Silver Springs, Florida. Ecol. Monogr. 27:55–112
- Oliver L, Fisher W, Ford S, Calvo LR, Burreson E, et al. 1998. *Perkinsus marinus* tissue distribution and seasonal variation in oysters *Crussostrea virginica* from Florida, Virginia and New York. *Dis. Aquat. Org.* 34:51–61
- Packman AI, Brooks NH. 2001. Hyporheic exchange of solutes and colloids with moving bed forms. Water Resour. Res. 37:2591–605
- Palacios SL, Zimmerman RC. 2007. Response of eelgrass Zostera marina to CO₂ enrichment: possible impacts of climate change and potential for remediation of coastal habitats. Mar. Ecol. Prog. Ser. 344:1–13
- Pamatmat MM. 1971. Oxygen consumption by the sea bed IV. Shipboard and laboratory experiments. *Limnol. Oceanogr.* 16:536–50
- Pamatmat MM, Fenton D. 1968. An instrument for measuring subtidal benthic metabolism in situ. *Limnol. Oceanogr.* 13:537–40

- Partch EN, Smith JD. 1978. Time dependent mixing in a salt wedge estuary. Estuar. Coast. Mar. Sci. 6:3-19
- Precht E, Franke U, Polerecky L, Huettel M. 2004. Oxygen dynamics in permeable sediments with wave-driven pore water exchange. *Limnol. Oceanogr.* 49:693–705
- Preziosi-Ribero A, Packman AI, Escobar-Vargas JA, Phillips CB, Donado LD, Arnon S. 2020. Fine sediment deposition and filtration under losing and gaining flow conditions: a particle tracking model approach. *Water Resour. Res.* 56:e2019WR026057
- Priestley CHB, Swinbank WC. 1947. Vertical transport of heat by turbulence in the atmosphere. *Proc. R. Soc.* A 189:543–61
- Raven J, Larkum A. 2007. Are there ecological implications for the proposed energetic restrictions on photosynthetic oxygen evolution at high oxygen concentrations? *Photosynth. Res.* 94:31–42
- Ray AJ, Aller RC. 1985. Physical irrigation of relict burrows: implications for sediment chemistry. Mar. Geol. 62:371–79
- Raymond P, Cole J. 2001. Gas exchange in rivers and estuaries: choosing a gas transfer velocity. *Estuaries* 24:312–17
- Reidenbach MA, Berg P, Hume A, Hansen JC, Whitman ER. 2013. Hydrodynamics of intertidal oyster reefs: the influence of boundary layer flow processes on sediment and oxygen exchange. *Limnol. Oceanogr. Fluids Environ.* 3:225–39
- Reimers CE, Fischer KM, Merewether R, Smith K, Jahnke RA. 1986. Oxygen microprofiles measured in situ in deep ocean sediments. *Nature* 320:741–44
- Reimers CE, Fogaren KE. 2021. Bottom boundary layer oxygen fluxes during winter on the Oregon shelf. J. Geophys. Res. Oceans 126:e2020JC016828
- Reimers CE, Özkan-Haller HT, Albright A, Berg P. 2016a. Microelectrode velocity effects and aquatic eddy covariance measurements under waves. J. Atmos. Ocean. Technol. 33:263–82
- Reimers CE, Özkan-Haller HT, Berg P, Devol A, McCann-Grosvenor K, Sanders RD. 2012. Benthic oxygen consumption rates during hypoxic conditions on the Oregon continental shelf: evaluation of the eddy correlation method. 7. Geophys. Res. 117:C02021
- Reimers CE, Özkan-Haller HT, Sanders RD, McCann-Grosvenor K, Chace PJ, Crowe SA. 2016b. The dynamics of benthic respiration at a mid-shelf station off Oregon. Aquat. Geochem. 22:505–27
- Reimers CE, Sanders RD, Dewey R, Noel R. 2020. Benthic fluxes of oxygen and heat from a seasonally hypoxic region of Saanich Inlet fjord observed by eddy covariance. *Estuar. Coast. Shelf Sci.* 243:106815
- Revsbech NP. 1989. An oxygen microsensor with a guard cathode. Limnol. Oceanogr. 34:474-78
- Reynolds O. 1895. IV. On the dynamical theory of incompressible viscous fluids and the determination of the criterion. *Philos. Trans. R. Soc. Lond. A* 186:123–64
- Rheuban JE, Berg P. 2013. The effects of spatial and temporal variability at the sediment surface on aquatic eddy correlation flux measurements. *Limnol. Oceanogr. Methods* 11:351–59
- Rheuban JE, Berg P, McGlathery KJ. 2014a. Ecosystem metabolism along a colonization gradient of eelgrass (*Zostera marina*) measured by eddy correlation. *Limnol. Oceanogr.* 59:1376–87
- Rheuban JE, Berg P, McGlathery KJ. 2014b. Multiple timescale processes drive ecosystem metabolism in eelgrass (*Zostera marina*) meadows. *Mar. Ecol. Prog. Ser.* 507:1–13
- Riisgård HU, Lüskow F, Pleissner D, Lundgreen K, López MAP. 2013. Effect of salinity on filtration rates of mussels *Mytilus edulis* with special emphasis on dwarfed mussels from the low-saline Central Baltic Sea. *Helgol. Mar. Res.* 67:591–98
- Rovelli L, Attard KM, Bryant LD, Flögel S, Stahl HJ, et al. 2015. Benthic O₂ uptake of two cold-water coral communities estimated with the non-invasive eddy-correlation technique. *Mar. Ecol. Prog. Ser.* 525:97–104
- Rusch A, Huettel M. 2000. Advective particle transport into permeable sediments—evidence from experiments in an intertidal sandflat. *Limnol. Oceanogr.* 45:525–33
- Rusch A, Huettel M, Forster S. 2000. Particulate organic matter in permeable marine sands—dynamics in time and depth. Estuar. Coast. Shelf Sci. 51:399–414
- Scrase FJ. 1930. Some Characteristics of Eddy Motion in the Atmosphere. London: Meteorol. Off.
- Short F. 1980. A simulation model of the seagrass production system. In Handbook of Seagrass Biology: An Ecosystem Perspective, ed. RC Phillips, CP McRoy, pp. 275–95. New York: Garland STPM

- Shumway SE, Koehn RK. 1982. Oxygen consumption in the American oyster Crassostrea virginica. Mar. Ecol. Prog. Ser. 9:59–68
- Smith SV. 1981. Marine macrophytes as a global carbon sink. Science 211:838-40
- Sorrell B, Dromgoole F. 1986. Errors in measurements of aquatic macrophyte gas exchange due to oxygen storage in internal airspaces. Aquat. Bot. 24:103–14
- Stratmann T, Soetaert K, Wei C-L, Lin Y-S, van Oevelen D. 2019. The SCOC database, a large, open, and global database with sediment community oxygen consumption rates. *Sci. Data* 6:242
- Swinbank WC. 1951. The measurement of vertical transfer of heat and water vapor by eddies in the lower atmosphere. 7. Meteorol. 8:115–45
- Tessmar-Raible K, Raible F, Arboleda E. 2011. Another place, another timer: marine species and the rhythms of life. *BioEssays* 33:165–72
- Thamdrup B. 2000. Bacterial manganese and iron reduction in aquatic sediments. *Adv. Microb. Ecol.* 16:41–84 Thibodeaux LJ, Boyle JD. 1987. Bedform-generated convective transport in bottom sediment. *Nature* 325:341–43
- Thomsen MS, McGlathery KJ, Tyler AC. 2006. Macroalgal distribution patterns in a shallow, soft-bottom lagoon, with emphasis on the nonnative *Gracilaria vermiculophylla* and *Godium fragile*. *Estuaries Coasts* 29:465–73
- Trowbridge J. 1998. On a technique for measurement of turbulent shear stress in the presence of surface waves. 7. Atmos. Ocean. Technol. 15:290–98
- Volaric MP, Berg P, Reidenbach MA. 2018. Oxygen metabolism of intertidal oyster reefs measured by aquatic eddy covariance. Mar. Ecol. Prog. Ser. 599:75–91
- Volaric MP, Berg P, Reidenbach MA. 2019. An invasive macroalga alters ecosystem metabolism and hydrodynamics on a tidal flat. Mar. Ecol. Prog. Ser. 628:1–16
- Volaric MP, Berg P, Reidenbach MA. 2020. Drivers of oyster reef ecosystem metabolism measured across multiple timescales. Estuaries Coasts 43:2034–45
- Wenzhofer F, Glud RN. 2004. Small-scale spatial and temporal variability in coastal benthic O₂ dynamics: effects of fauna activity. *Limnol. Oceanogr.* 49:1471–81



Annual Review of Marine Science

Volume 14, 2022

Contents

The Goldilocks Principle: A Unifying Perspective on Biochemical Adaptation to Abiotic Stressors in the Sea George N. Somero	1
Physiological Consequences of Oceanic Environmental Variation: Life from a Pelagic Organism's Perspective Mark W. Denny and W. Wesley Dowd	25
The Balance of Nature: A Global Marine Perspective Constantin W. Arnscheidt and Daniel H. Rothman	49
Ecological Leverage Points: Species Interactions Amplify the Physiological Effects of Global Environmental Change in the Ocean Kristy J. Kroeker and Eric Sanford	75
The Biological Effects of Pharmaceuticals in the Marine Environment Marica Mezzelani and Francesco Regoli	105
The Functional and Ecological Significance of Deep Diving by Large Marine Predators Camrin D. Braun, Martin C. Arostegui, Simon R. Thorrold, Yannis P. Papastamatiou, Peter Gaube, Jorge Fontes, and Pedro Afonso	129
Environmental DNA Metabarcoding: A Novel Method for Biodiversity Monitoring of Marine Fish Communities Masaki Miya	161
The Enzymology of Ocean Global Change David A. Hutchins and Sergio A. Sañudo-Wilhelmy	187
Using Chlorophyll Fluorescence to Determine the Fate of Photons Absorbed by Phytoplankton in the World's Oceans Maxim Y. Gorbunov and Paul G. Falkowski	213
Temporal and Spatial Signaling Mediating the Balance of the Plankton Microbiome Yun Deng, Marine Vallet, and Georg Pohnert	239
The Physiology and Biogeochemistry of SUP05 Robert M. Morris and Rachel L. Spietz	

Machine Learning for the Study of Plankton and Marine Snow from Images Jean-Olivier Irisson, Sakina-Dorothée Ayata, Dhugal J. Lindsay, Lee Karp-Boss, and Lars Stemmann	. 277
Earth, Wind, Fire, and Pollution: Aerosol Nutrient Sources and Impacts on Ocean Biogeochemistry Douglas S. Hamilton, Morgane M.G. Perron, Tami C. Bond, Andrew R. Bowie, Rebecca R. Buchholz, Cecile Guieu, Akinori Ito, Willy Maenhaut, Stelios Myriokefalitakis, Nazlı Olgun, Sagar D. Rathod, Kerstin Schepanski, Alessandro Tagliabue, Robert Wagner, and Natalie M. Mahowald	303
The History of Ocean Oxygenation Christopher T. Reinhard and Noah J. Planavsky	331
Organic Matter Supply and Utilization in Oxygen Minimum Zones Anja Engel, Rainer Kiko, and Marcus Dengler	355
Argo—Two Decades: Global Oceanography, Revolutionized Gregory C. Johnson, Shigeki Hosoda, Steven R. Jayne, Peter R. Oke, Stephen C. Riser, Dean Roemmich, Tohsio Suga, Virginie Thierry, Susan E. Wijffels, and Jianping Xu	379
Ventilation of the Southern Ocean Pycnocline Adele K. Morrison, Darryn W. Waugh, Andrew McC. Hogg, Daniel C. Jones, and Ryan P. Abernathey	405
Aquatic Eddy Covariance: The Method and Its Contributions to Defining Oxygen and Carbon Fluxes in Marine Environments Peter Berg, Markus Huettel, Ronnie N. Glud, Clare E. Reimers, and Karl M. Attard	431
Modeling the Morphodynamics of Coastal Responses to Extreme Events: What Shape Are We In? Christopher R. Sherwood, Ap van Dongeren, James Doyle, Christie A. Hegermiller, Tian-Jian Hsu, Tarandeep S. Kalra, Maitane Olabarrieta, Allison M. Penko, Yashar Rafati, Dano Roelvink, Marlies van der Lugt, Jay Veeramony, and John C. Warner	. 457

Errata

An online log of corrections to *Annual Review of Marine Science* articles may be found at http://www.annualreviews.org/errata/marine